

J/ψ production at high transverse momenta in $p+p$ and Au+Au collisions at $\sqrt{s_{\text{NN}}} = 200$ GeV

L. Adamczyk,¹ G. Agakishiev,²¹ M. M. Aggarwal,³³ Z. Ahammed,⁵¹ A. V. Alakhverdyants,²¹ I. Alekseev,¹⁹ J. Alford,²² B. D. Anderson,²² C. D. Anson,³⁰ D. Arkhipkin,⁴ E. Aschenauer,⁴ G. S. Averichev,²¹ J. Balewski,²⁶ A. Banerjee,⁵¹ Z. Barnovska,¹⁴ D. R. Beavis,⁴ R. Bellwied,⁴⁷ M. J. Betancourt,²⁶ R. R. Betts,¹⁰ A. Bhasin,²⁰ A. K. Bhati,³³ H. Bichsel,⁵³ J. Bielcik,¹³ J. Bielcikova,¹⁴ L. C. Bland,⁴ I. G. Bordyuzhin,¹⁹ W. Borowski,⁴⁴ J. Bouchet,²² A. V. Brandin,²⁹ S. G. Brovko,⁶ E. Bruna,⁵⁵ S. Bültmann,³¹ I. Bunzarov,²¹ T. P. Burton,⁴ J. Butterworth,³⁹ X. Z. Cai,⁴³ H. Caines,⁵⁵ M. Calderón de la Barca Sánchez,⁶ D. Cebra,⁶ R. Cendejas,⁷ M. C. Cervantes,⁴⁵ P. Chaloupka,¹⁴ Z. Chang,⁴⁵ S. Chattopadhyay,⁵¹ H. F. Chen,⁴¹ J. H. Chen,⁴³ J. Y. Chen,⁹ L. Chen,⁹ J. Cheng,⁴⁸ M. Cherney,¹² A. Chikanian,⁵⁵ W. Christie,⁴ P. Chung,¹⁴ J. Chwastowski,¹¹ M. J. M. Coddington,⁴⁵ R. Corliss,²⁶ J. G. Cramer,⁵³ H. J. Crawford,⁵ X. Cui,⁴¹ A. Davila Leyva,⁴⁶ L. C. De Silva,⁴⁷ R. R. Debbé,⁴ T. G. Dedovich,²¹ J. Deng,⁴² R. Derradi de Souza,⁸ S. Dhamija,¹⁸ L. Didenko,⁴ F. Ding,⁶ A. Dion,⁴ P. Djawotho,⁴⁵ X. Dong,²⁵ J. L. Drachenberg,⁴⁵ J. E. Draper,⁶ C. M. Du,²⁴ L. E. Dunkelberger,⁷ J. C. Dunlop,⁴ L. G. Efimov,²¹ M. Elnimr,⁵⁴ J. Engelage,⁵ G. Eppley,³⁹ L. Eun,²⁵ O. Evdokimov,¹⁰ R. Fatemi,²³ S. Fazio,⁴ J. Fedorisin,²¹ R. G. Fersch,²³ P. Filip,²¹ E. Finch,⁵⁵ Y. Fisyak,⁴ C. A. Gagliardi,⁴⁵ D. R. Gangadharan,³⁰ F. Geurts,³⁹ A. Gibson,⁵⁰ S. Gliske,² Y. N. Gorbunov,¹² O. G. Grebenyuk,²⁵ D. Grosnick,⁵⁰ S. Gupta,²⁰ W. Guryn,⁴ B. Haag,⁶ O. Hajkova,¹³ A. Hamed,⁴⁵ L.-X. Han,⁴³ J. W. Harris,⁵⁵ J. P. Hays-Wehle,²⁶ S. Heppelmann,³⁴ A. Hirsch,³⁶ G. W. Hoffmann,⁴⁶ D. J. Hofman,¹⁰ S. Horvat,⁵⁵ B. Huang,⁴ H. Z. Huang,⁷ P. Huck,⁹ T. J. Humanic,³⁰ L. Huo,⁴⁵ G. Igo,⁷ W. W. Jacobs,¹⁸ C. Jena,¹⁶ J. Joseph,²² E. G. Judd,⁵ S. Kabana,⁴⁴ K. Kang,⁴⁸ J. Kapitan,¹⁴ K. Kauder,¹⁰ H. W. Ke,⁹ D. Keane,²² A. Kechechyan,²¹ A. Kesich,⁶ D. Kettler,⁵³ D. P. Kikola,³⁶ J. Kiryluk,²⁵ I. Kisel,²⁵ A. Kisiel,⁵² V. Kizka,²¹ S. R. Klein,²⁵ D. D. Koetke,⁵⁰ T. Kollegger,¹⁵ J. Konzer,³⁶ I. Koralt,³¹ L. Koroleva,¹⁹ W. Korsch,²³ L. Kotchenda,²⁹ P. Kravtsov,²⁹ K. Krueger,² I. Kulakov,²⁵ L. Kumar,²² M. A. C. Lamont,⁴ J. M. Landgraf,⁴ S. LaPointe,⁵⁴ J. Lauret,⁴ A. Lebedev,⁴ R. Lednicky,²¹ J. H. Lee,⁴ W. Leight,²⁶ M. J. LeVine,⁴ C. Li,⁴¹ L. Li,⁴⁶ W. Li,⁴³ X. Li,³⁶ X. Li,⁴² Y. Li,⁴⁸ Z. M. Li,⁹ L. M. Lima,⁴⁰ M. A. Lisa,³⁰ F. Liu,⁹ T. Ljubicic,⁴ W. J. Llope,³⁹ R. S. Longacre,⁴ Y. Lu,⁴¹ X. Luo,⁹ A. Luszczak,¹¹ G. L. Ma,⁴³ Y. G. Ma,⁴³ D. M. M. D. Madagadagettige Don,¹² D. P. Mahapatra,¹⁶ R. Majka,⁵⁵ O. I. Mall,⁶ S. Margetis,²² C. Markert,⁴⁶ H. Masui,²⁵ H. S. Matis,²⁵ D. McDonald,³⁹ T. S. McShane,¹² S. Mioduszewski,⁴⁵ M. K. Mitrovski,⁴ Y. Mohammed,⁴⁵ B. Mohanty,⁵¹ M. M. Mondal,⁴⁵ B. Morozov,¹⁹ M. G. Munhoz,⁴⁰ M. K. Mustafa,³⁶ M. Naglis,²⁵ B. K. Nandi,¹⁷ Md. Nasim,⁵¹ T. K. Nayak,⁵¹ J. M. Nelson,³ L. V. Nogach,³⁵ J. Novak,²⁸ G. Odyniec,²⁵ A. Ogawa,⁴ K. Oh,³⁷ A. Ohlson,⁵⁵ V. Okorokov,²⁹ E. W. Oldag,⁴⁶ R. A. N. Oliveira,⁴⁰ D. Olson,²⁵ P. Ostrowski,⁵² M. Pachr,¹³ B. S. Page,¹⁸ S. K. Pal,⁵¹ Y. X. Pan,⁷ Y. Pandit,²² Y. Panebratsev,²¹ T. Pawlak,⁵² B. Pawlik,³² H. Pei,¹⁰ C. Perkins,⁵ W. Peryt,⁵² P. Pile,⁴ M. Planinic,⁵⁶ J. Pluta,⁵² D. Plyku,³¹ N. Poljak,⁵⁶ J. Porter,²⁵ A. M. Poskanzer,²⁵ C. B. Powell,²⁵ D. Prindle,⁵³ C. Pruneau,⁵⁴ N. K. Pruthi,³³ M. Przybycien,¹ P. R. Pujahari,¹⁷ J. Putschke,⁵⁴ H. Qiu,²⁵ R. Raniwala,³⁸ S. Raniwala,³⁸ R. L. Ray,⁴⁶ R. Redwine,²⁶ R. Reed,⁶ C. K. Riley,⁵⁵ H. G. Ritter,²⁵ J. B. Roberts,³⁹ O. V. Rogachevskiy,²¹ J. L. Romero,⁶ J. F. Ross,¹² L. Ruan,⁴ J. Rusnak,¹⁴ N. R. Sahoo,⁵¹ I. Sakrejda,²⁵ S. Salur,²⁵ A. Sandacz,⁵² J. Sandweiss,⁵⁵ E. Sangaline,⁶ A. Sarkar,¹⁷ J. Schambach,⁴⁶ R. P. Scharenberg,³⁶ A. M. Schmah,²⁵ B. Schmidke,⁴ N. Schmitz,²⁷ T. R. Schuster,¹⁵ J. Seele,²⁶ J. Seger,¹² P. Seyboth,²⁷ N. Shah,⁷ E. Shabaliev,²¹ M. Shao,⁴¹ B. Sharma,³³ M. Sharma,⁵⁴ S. S. Shi,⁹ Q. Y. Shou,⁴³ E. P. Sichtermann,²⁵ R. N. Singaraju,⁵¹ M. J. Skoby,¹⁸ D. Smirnov,⁴ N. Smirnov,⁵⁵ D. Solanki,³⁸ P. Sorensen,⁴ U. G. deSouza,⁴⁰ H. M. Spinka,² B. Srivastava,³⁶ T. D. S. Stanislaus,⁵⁰ S. G. Steadman,²⁶ J. R. Stevens,¹⁸ R. Stock,¹⁵ M. Strikhanov,²⁹ B. Stringfellow,³⁶ A. A. P. Suaide,⁴⁰ M. C. Suarez,¹⁰ M. Sumner,¹⁴ X. M. Sun,²⁵ Y. Sun,⁴¹ Z. Sun,²⁴ B. Surrow,²⁶ D. N. Svirida,¹⁹ T. J. M. Symons,²⁵ A. Szanto de Toledo,⁴⁰ J. Takahashi,⁸ A. H. Tang,⁴ Z. Tang,⁴¹ L. H. Tarini,⁵⁴ T. Tarnowsky,²⁸ D. Thein,⁴⁶ J. H. Thomas,²⁵ J. Tian,⁴³ A. R. Timmins,⁴⁷ D. Tlusty,¹⁴ M. Tokarev,²¹ T. A. Trainor,⁵³ S. Trentalange,⁷ R. E. Tribble,⁴⁵ P. Tribedy,⁵¹ B. A. Trzeciak,⁵² O. D. Tsai,⁷ J. Turnau,³² T. Ullrich,⁴ D. G. Underwood,² G. Van Buren,⁴ G. van Nieuwenhuizen,²⁶ J. A. Vanfossen, Jr.,²² R. Varma,¹⁷ G. M. S. Vasconcelos,⁸ F. Videbæk,⁴ Y. P. Viyogi,⁵¹ S. Vokal,²¹ S. A. Voloshin,⁵⁴ A. Vossen,¹⁸ M. Wada,⁴⁶ F. Wang,³⁶ G. Wang,⁷ H. Wang,²⁸ J. S. Wang,²⁴ Q. Wang,³⁶ X. L. Wang,⁴¹ Y. Wang,⁴⁸ G. Webb,²³ J. C. Webb,⁴ G. D. Westfall,²⁸ C. Whitten Jr.,⁷ H. Wieman,²⁵ S. W. Wissink,¹⁸ R. Witt,⁴⁹ W. Witzke,²³ Y. F. Wu,⁹ Z. Xiao,⁴⁸ W. Xie,³⁶ K. Xin,³⁹ H. Xu,²⁴ N. Xu,²⁵ Q. H. Xu,⁴² W. Xu,⁷ Y. Xu,⁴¹ Z. Xu,⁴ L. Xue,⁴³ Y. Yang,²⁴ Y. Yang,⁹ P. Yepes,³⁹ Y. Yi,³⁶ K. Yip,⁴ I.-K. Yoo,³⁷

M. Zawisza,⁵² H. Zbroszczyk,⁵² J. B. Zhang,⁹ S. Zhang,⁴³ W. M. Zhang,²² X. P. Zhang,⁴⁸ Y. Zhang,⁴¹
Z. P. Zhang,⁴¹ F. Zhao,⁷ J. Zhao,⁴³ C. Zhong,⁴³ X. Zhu,⁴⁸ Y. H. Zhu,⁴³ Y. Zoulkarneeva,²¹ and M. Zyzak²⁵

(STAR Collaboration)

- ¹AGH University of Science and Technology, Cracow, Poland
- ²Argonne National Laboratory, Argonne, Illinois 60439, USA
- ³University of Birmingham, Birmingham, United Kingdom
- ⁴Brookhaven National Laboratory, Upton, New York 11973, USA
- ⁵University of California, Berkeley, California 94720, USA
- ⁶University of California, Davis, California 95616, USA
- ⁷University of California, Los Angeles, California 90095, USA
- ⁸Universidade Estadual de Campinas, Sao Paulo, Brazil
- ⁹Central China Normal University (HZNU), Wuhan 430079, China
- ¹⁰University of Illinois at Chicago, Chicago, Illinois 60607, USA
- ¹¹Cracow University of Technology, Cracow, Poland
- ¹²Creighton University, Omaha, Nebraska 68178, USA
- ¹³Czech Technical University in Prague, FNSPE, Prague, 115 19, Czech Republic
- ¹⁴Nuclear Physics Institute AS CR, 250 68 Řež/Prague, Czech Republic
- ¹⁵University of Frankfurt, Frankfurt, Germany
- ¹⁶Institute of Physics, Bhubaneswar 751005, India
- ¹⁷Indian Institute of Technology, Mumbai, India
- ¹⁸Indiana University, Bloomington, Indiana 47408, USA
- ¹⁹Alikhanov Institute for Theoretical and Experimental Physics, Moscow, Russia
- ²⁰University of Jammu, Jammu 180001, India
- ²¹Joint Institute for Nuclear Research, Dubna, 141 980, Russia
- ²²Kent State University, Kent, Ohio 44242, USA
- ²³University of Kentucky, Lexington, Kentucky, 40506-0055, USA
- ²⁴Institute of Modern Physics, Lanzhou, China
- ²⁵Lawrence Berkeley National Laboratory, Berkeley, California 94720, USA
- ²⁶Massachusetts Institute of Technology, Cambridge, MA 02139-4307, USA
- ²⁷Max-Planck-Institut für Physik, Munich, Germany
- ²⁸Michigan State University, East Lansing, Michigan 48824, USA
- ²⁹Moscow Engineering Physics Institute, Moscow Russia
- ³⁰Ohio State University, Columbus, Ohio 43210, USA
- ³¹Old Dominion University, Norfolk, VA, 23529, USA
- ³²Institute of Nuclear Physics PAN, Cracow, Poland
- ³³Panjab University, Chandigarh 160014, India
- ³⁴Pennsylvania State University, University Park, Pennsylvania 16802, USA
- ³⁵Institute of High Energy Physics, Protvino, Russia
- ³⁶Purdue University, West Lafayette, Indiana 47907, USA
- ³⁷Pusan National University, Pusan, Republic of Korea
- ³⁸University of Rajasthan, Jaipur 302004, India
- ³⁹Rice University, Houston, Texas 77251, USA
- ⁴⁰Universidade de Sao Paulo, Sao Paulo, Brazil
- ⁴¹University of Science & Technology of China, Hefei 230026, China
- ⁴²Shandong University, Jinan, Shandong 250100, China
- ⁴³Shanghai Institute of Applied Physics, Shanghai 201800, China
- ⁴⁴SUBATECH, Nantes, France
- ⁴⁵Texas A&M University, College Station, Texas 77843, USA
- ⁴⁶University of Texas, Austin, Texas 78712, USA
- ⁴⁷University of Houston, Houston, TX, 77204, USA
- ⁴⁸Tsinghua University, Beijing 100084, China
- ⁴⁹United States Naval Academy, Annapolis, MD 21402, USA
- ⁵⁰Valparaiso University, Valparaiso, Indiana 46383, USA
- ⁵¹Variable Energy Cyclotron Centre, Kolkata 700064, India
- ⁵²Warsaw University of Technology, Warsaw, Poland
- ⁵³University of Washington, Seattle, Washington 98195, USA
- ⁵⁴Wayne State University, Detroit, Michigan 48201, USA
- ⁵⁵Yale University, New Haven, Connecticut 06520, USA
- ⁵⁶University of Zagreb, Zagreb, HR-10002, Croatia

(Dated: March 22, 2019)

We report J/ψ spectra for transverse momenta $p_T > 5$ GeV/c at mid-rapidity in $p+p$ and Au+Au collisions at $\sqrt{s_{NN}} = 200$ GeV. The inclusive J/ψ spectrum and the extracted B -hadron feed-down

are compared to models incorporating different production mechanisms. We observe significant suppression of the J/ψ yields for $p_T > 5$ GeV/ c in 0-30% Au+Au collisions relative to the $p+p$ yield scaled by the number of binary nucleon-nucleon collisions in Au+Au collisions. In 30-60% collisions, no such suppression is observed. The level of suppression is consistently less than that of high- p_T π^\pm and low- p_T J/ψ .

PACS numbers: 12.38.Mh, 14.40.Gx, 25.75.Dw, 25.75.Nq

Ultrarelativistic heavy-ion collisions provide a unique environment to study strongly interacting matter at high temperature and energy density where a transition from the hadronic phase of matter to a new partonic phase, the Quark-Gluon Plasma (QGP), takes place. Measurements of the in-medium dissociation probability of the different quarkonium states are expected to provide an estimate of the initial temperature of the system [1–5]. The $J/\psi(1S)$ is the lightest and most abundantly produced quarkonium state accessible in experiment. However, significant decay contributions ($> 40\%$) from excited $c\bar{c}$ states, such as the χ_c and $\psi(2S)$, and from B mesons could complicate the suppression picture suggested by direct dissociation models [6]. In addition, other effects absent in $p+p$ collisions are likely to have a significant impact on the observed J/ψ yields in relativistic heavy-ion collisions at CERN-SPS, BNL-RHIC and CERN-LHC [7–11]. These effects include cold nuclear matter (CNM) effects such as initial state parton scattering, nuclear shadowing and nuclear absorption, the combined effects of finite J/ψ formation time and the finite space-time extent of the hot, dense volume where the dissociation can occur, and recombination of unassociated c and \bar{c} in the medium [12]. Most of these effects are expected to decrease with increasing J/ψ p_T [13, 14]. It is therefore anticipated that J/ψ measurements at high- p_T provide an important tool to decouple some of the mechanisms mentioned above and provide a cleaner way to extract the contribution from color-screening effects [13–16]. STAR’s previous J/ψ measurements are consistent with no suppression for $p_T > 5$ GeV/ c in Cu+Cu collisions at $\sqrt{s_{NN}} = 200$ GeV, to within the limited precision of the data [17]. In addition, the small system size created in Cu+Cu collisions may result in high- p_T J/ψ formation outside the medium. Precise measurements in Au+Au collisions are thus crucial for a systematic study of J/ψ production in the hot, dense medium.

The interpretation of medium-induced J/ψ modification requires a good understanding of its production mechanisms in $p+p$ collisions, which include direct production via gluon fusion, parton fragmentation, and feed-down from higher charmonium states and B -hadron decays [6]. The initial hard interactions required to create the charm quark pairs can be well calculated in perturbative QCD (pQCD). However, the subsequent soft processes required to form the J/ψ hadron and the J/ψ formation time are theoretically not well understood [6]. No model at present fully explains the J/ψ observations

in elementary collisions [6]. The J/ψ spectrum in the intermediate and high- p_T range, together with the angular correlations of a high- p_T J/ψ and associated charged hadrons, may provide additional insights in the underlying production mechanisms.

In this letter, we report a measurement of J/ψ production for $2 < p_T < 14$ GeV/ c in $p+p$ and Au+Au collisions at $\sqrt{s_{NN}} = 200$ GeV. The inclusive J/ψ cross sections at mid-rapidity ($|y| < 1$) in $p+p$ and Au+Au collisions are presented. The nuclear modification factor, R_{AA} – the ratio of the yield in Au+Au to that in $p+p$ collisions scaled by the number of underlying binary nucleon-nucleon collisions – is calculated and compared to theoretical calculations.

The Au+Au data used for this analysis were recorded in 2010, and the $p+p$ data in 2009. The minimum bias (MB) trigger was defined to be a coincidence of the two Vertex Position Detectors (VPD) [18]. Online trigger conditions that utilized a MB trigger condition and two thresholds for the energy deposited in any single Barrel Electromagnetic Calorimeter (BEMC) [19] tower, with a size of $\Delta\eta \times \Delta\phi = 0.05 \times 0.05$, were used to maximize the sampled luminosity. To increase the trigger efficiency, the $p+p$ data with high BEMC threshold were recorded without a MB requirement. The $p+p$ data with low BEMC threshold were pre-scaled to keep the data rate manageable. The integrated luminosities of the data samples used for this analysis are 23.1 pb^{-1} and 1.8 pb^{-1} with a transverse energy threshold of $E_T > 6.0$ and 2.6 GeV, respectively, in $p+p$ collisions and 1.4 nb^{-1} with $E_T > 4.3$ GeV in Au+Au collisions. In the Au+Au data, the collision centrality is determined by the distribution of charged-particle multiplicity within $|\eta| < 0.5$ and Monte Carlo Glauber calculations [20].

In this analysis, $J/\psi \rightarrow e^+e^-$ decays were reconstructed using the STAR Time Projection Chamber (TPC) [22] and the BEMC [19] with full azimuthal coverage over the pseudorapidity range $|\eta| < 1$ [17, 23]. Electron identification (eID) for the BEMC triggered tracks was achieved by measuring the ionization energy loss (dE/dx) and track momentum from the TPC, as well as the energy deposition in the BEMC. In addition, the shower profile in the barrel shower maximum detector (BSMD) [19] was used in Au+Au collisions to further suppress hadron contamination. At moderate p_T ($1 \lesssim p_T \lesssim 3$ GeV/ c), TPC dE/dx provides eID with reasonable efficiency and purity. At low p_T ($0.2 < p_T \lesssim 3$ GeV/ c), the eID significantly benefits

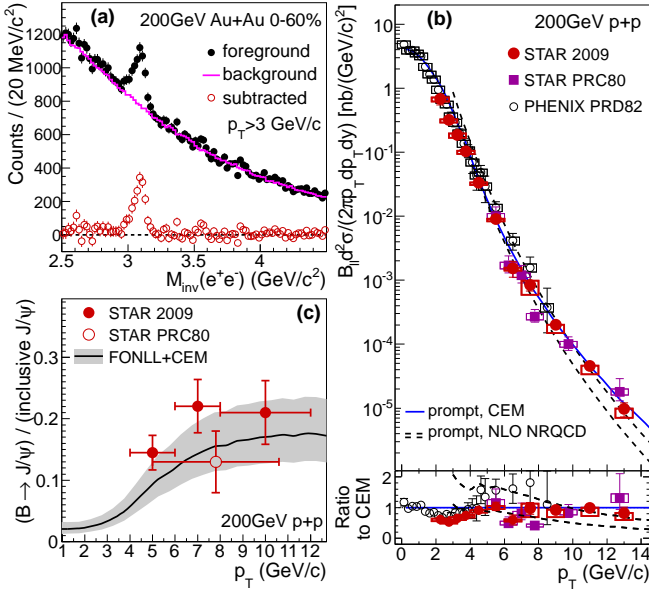


FIG. 1: (Color online.) (a) The unlike-sign e^+e^- invariant mass distribution from same-event pairs (filled circles) and mixed-event pairs (continuous curve) and their difference (open circles) in Au+Au collisions at $\sqrt{s_{NN}} = 200$ GeV. (b) The invariant J/ψ cross section versus p_T in p+p collisions at $\sqrt{s} = 200$ GeV. The vertical bars and boxes depict the statistical and systematic uncertainties, respectively. Also shown are results published by STAR [17] and PHENIX [21]. The curves are theoretical calculations described in the text. (c) The fraction of $B \rightarrow J/\psi$ over the inclusive J/ψ yield in p+p collisions. The FONLL+CEM model calculation is also shown.

from a recently installed large area time-of-flight (TOF) detector covering $|\eta| < 0.9$ [24–26]. The complete TOF detector was available for the 2010 Au+Au run, whereas 72% was available for the p+p data collected in 2009.

The J/ψ signal was extracted by subtracting from the unlike-sign ee invariant mass spectrum the random combinatorial background that was reproduced by the like-sign spectrum in p+p collisions and unlike-sign spectrum from mixed-events in Au+Au collisions [27]. Figure 1(a) shows the invariant mass distribution before and after the combinatorial background subtraction in Au+Au collisions at $\sqrt{s_{NN}} = 200$ GeV. The J/ψ raw yields were obtained from a mass window of $2.7 < M_{inv}^{ee} < 3.3 - 3.4$ GeV/c^2 in p+p collisions depending on the J/ψ p_T , and $2.9 < M_{inv}^{ee} < 3.2$ GeV/c^2 in Au+Au collisions. The yields were corrected for $\approx 10\%$ radiation losses that cause some of the decay daughters to be reconstructed with M_{inv}^{ee} outside the above mass ranges. The total J/ψ yield was ≈ 1100 ($p_T > 2$ GeV/c) in p+p collisions. It was ≈ 1000 and 300 ($p_T > 3$ GeV/c) in 0-20% and 40-60% Au+Au collisions, respectively. The signal to background ratio (S/B) was ≈ 4 in p+p collisions and $\approx 1/7$ ($1/2$) in 0-20% (40-60%) Au+Au collisions. In the J/ψ -hadron correlation analysis, the cuts were selected to provide a

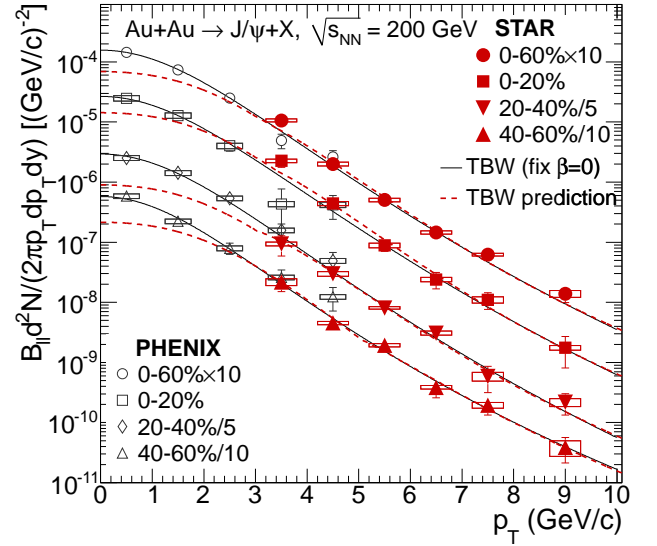


FIG. 2: (Color online) J/ψ p_T distributions in Au+Au collisions with different centralities at $\sqrt{s_{NN}} = 200$ GeV. For clarity, the data and curves have been scaled as indicated in the legends. The PHENIX results are reported in [8]. The curves are model fits described in the text.

high S/B ratio. About 400 J/ψ with $p_T > 4$ GeV/c and $3.0 < M_{inv}^{ee} < 3.2$ GeV/c^2 were observed with a S/B ratio of 22/1 in p+p collisions [28].

Acceptance and efficiency corrections were studied using Monte Carlo GEANT simulations [20]. The systematic uncertainties are due to kinematic cuts ($< 12\%$), signal extraction (including the contribution from correlated background, 2-26%), momentum resolution ($< 3\%$), and efficiency (7.5%). The normalization uncertainty for the cross section in p+p collisions is 8.1% [29]. The correlation of the systematic uncertainties in the spectra was taken into account in evaluating the uncertainty on R_{AA} .

Figure 1(b) shows the J/ψ invariant cross section times the branching ratio (B_I) [30] as a function of p_T for p+p collisions at $\sqrt{s} = 200$ GeV. The new results are consistent with those previously published by STAR [17] and PHENIX [21]. The rapidity window for PHENIX results is $|y| < 0.35$. The dashed curves depict next-to-leading order (NLO) theoretical Non-Relativistic QCD (NRQCD) calculations from color-octet (CO) and color-singlet (CS) transitions [31] for prompt J/ψ production in p+p collisions. The CS+CO calculations match the p_T spectra for $p_T > 4$ GeV/c to within the uncertainties. The continuous curve shows the calculation from the color evaporation model (CEM) for prompt J/ψ [32]. It describes the p_T spectra reasonably well. The bottom panel shows the ratios of the data and theory calculations to the CEM calculation. A model based on NNLO* CS [33] predicts a too steep p_T dependence, as discussed in [17].

The relative contribution of B -hadron feed-down to the inclusive J/ψ yield was obtained in the same way as

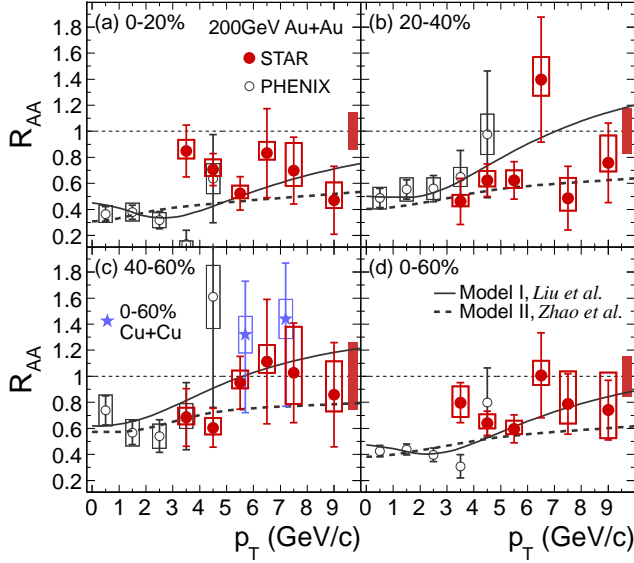


FIG. 3: (Color online.) J/ψ R_{AA} versus p_T for several centrality bins for Au+Au collisions at $\sqrt{s_{NN}} = 200$ GeV. The statistical (systematic) uncertainties are shown with vertical bars (open boxes). The filled boxes about unity on the right show the size of the normalization uncertainty. PHENIX low- p_T J/ψ results [8] and STAR high- p_T results in Cu+Cu collisions [17] are shown for comparison. The curves are the predictions by Model I (Liu et al.) [13] and Model II (Zhao et al.) [14].

in [17, 23]. We note that this method is data-driven, although it relies also on the validity of PYTHIA's [34, 35] modeling of the near-side associated hadron distributions. The effect is found to be 10-25% for $4 < p_T < 12$ GeV/c as shown in Fig. 1(c). Within errors our data are consistent with the Fixed Order plus Next-to-Leading Logarithms (FONLL) plus CEM prediction [36, 37] indicated by the curve and uncertainty band. More precise measurements using displaced vertex techniques [38, 39] similar to those employed by CDF in $p + \bar{p}$ collisions at $\sqrt{s} = 1.96$ TeV and by ATLAS and CMS in $p+p$ collisions at $\sqrt{s} = 7$ TeV [40–42] are needed to quantify the anticipated energy dependence [36, 37].

The measured J/ψ p_T spectra in Au+Au collisions for different centralities are shown in Fig. 2, and are consistent with the low- p_T J/ψ results from PHENIX in the region of overlap in p_T . The continuous curves depict fits based on the Tsallis statistics Blast-wave (TBW) model to the combined STAR and PHENIX data with the radial flow velocity β fixed to zero [43]. The fits reproduce the data reasonably well. Under the assumption that the J/ψ flows like light hadrons [43, 44], the TBW calculations shown as dashed curves underpredict the yields at low p_T . This could be due to a small (or zero) radial flow or a significant contribution from charm quark recombination that would enhance the yield at low p_T , or both.

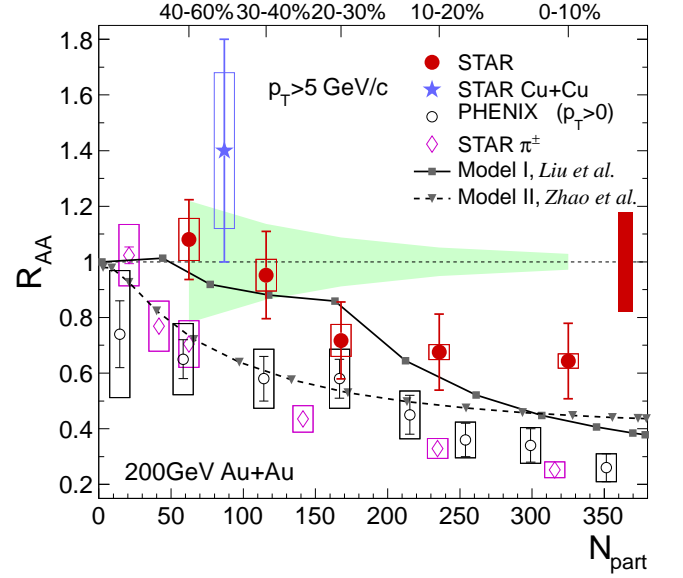


FIG. 4: (Color online) R_{AA} versus N_{part} for high- p_T J/ψ , low- p_T J/ψ from PHENIX [8], and high- p_T π^\pm from STAR [45, 46]. The statistical (systematic) uncertainties are shown in vertical bars (boxes). The shaded green band about unity shows the systematic uncertainties from N_{bin} and the box about unity on the right shows the R_{AA} normalization uncertainty from the statistical and global systematic uncertainties of the $p+p$ reference data.

Figure 3 shows the J/ψ R_{AA} versus p_T for different centrality bins. The STAR Cu+Cu J/ψ results [17] are also shown. For $p_T > 5$ GeV/c, J/ψ R_{AA} in the 40-60% centrality bin is consistent with unity and with our previous measurement in Cu+Cu collisions with a similar average number of participants (N_{part}). The curves show two theoretical calculations [13, 14] describing the data reasonably well. These calculations include contributions from prompt production and statistical charm quark regeneration. The suppression of the prompt J/ψ component in the model calculations is mainly due to the color-screening effect. The model from Zhao et al. (Model II) [14] also includes the J/ψ formation-time effect and the B -hadron feed-down contribution.

For $p_T > 5$ GeV/c, J/ψ production follows the scaling of the cross section, $E \frac{d^3\sigma}{dp^3} = g(x_T)/(\sqrt{s})^n$, with $x_T = 2p_T/\sqrt{s}$ [47, 48] observed in $p+p$ collisions at $\sqrt{s} = 200$ GeV [17]. This indicates that soft processes do not alter high- p_T J/ψ production. In this p_T region, the CNM and $c\bar{c}$ recombination effects are expected to be negligible in heavy-ion collisions [13, 14], and AdS/CFT predicts suppression in the QGP for direct J/ψ [15].

We present high- p_T ($p_T > 5$ GeV/c) R_{AA} as a function of N_{part} in Fig. 4. No significant suppression of high- p_T J/ψ production is observed in mid-central to peripheral collisions (30-60%, $N_{part} \lesssim 140$). In central collisions (0-30%, $N_{part} \gtrsim 140$), high- p_T J/ψ are significantly sup-

pressed. The R_{AA} of low- p_T ($0 < p_T < 5$ GeV/c) J/ψ measured by PHENIX [8] and high- p_T ($p_T > 5$ GeV/c) charged pions measured by STAR [45, 46] are shown for comparison [8, 45, 46]. The high- p_T J/ψ R_{AA} is systematically higher. The predictions of high- p_T J/ψ R_{AA} from Model I (Liu et al.) [49] and Model II (Zhao et al.) [14] are shown as continuous and dashed curves, respectively. Model I describes our data reasonably well. Model II underpredicts J/ψ R_{AA} at $N_{part} > 70$.

The high- p_T J/ψ R_{AA} versus centrality is different from that of high- p_T pions. This is expected from differences in their production. Dissociation is considered to be the dominant mechanism in the case of J/ψ production, and induced gluon radiation in the case of pion production. For $p_T > 5$ GeV/c, the recombination and initial parton scattering effects are expected to be negligible [13, 14]. The observed J/ψ R_{AA} dependence on p_T and system size might be due to the interplay of formation time, color screening, sequential suppression, and parton distribution functions in heavy nuclei [12]. Future J/ψ measurements in d +Au collisions over a broad range in p_T are needed to understand the CNM effects at RHIC. The B -hadron feed-down contribution is assumed to be the same in Au+Au and p + p collisions. Based on our measurement, R_{AA} for prompt J/ψ with $p_T > 5$ GeV/c in the most central collisions will be 0.80 if B -hadrons are completely suppressed and 0.55 if B -hadrons are unsuppressed.

In summary, we report measurements of J/ψ production in $\sqrt{s_{NN}} = 200$ GeV p + p and Au+Au collisions for $p_T > 2 - 3$ GeV/c at RHIC. The p_T spectrum in p + p collisions is compared to various theoretical calculations. Currently, only the CEM model and NLO CS+CO calculation describe our data. Based on the measurement of azimuthal correlations between high- p_T J/ψ and charged hadrons we estimate the fraction of J/ψ from B -hadron decay to be 10-25% in the p_T range of 4-12 GeV/c in p + p collisions. The nuclear modification factor R_{AA} in Au+Au increases from low to high p_T . For $p_T > 5$ GeV/c, J/ψ R_{AA} is consistent with no suppression from mid-central to peripheral collisions (30-60% centrality), and significantly smaller than unity in the most central Au+Au collisions. The results on R_{AA} versus p_T and N_{part} provide new insight in the study of color screening features for charmonium.

We thank the RHIC Operations Group and RCF at BNL, the NERSC Center at LBNL and the Open Science Grid consortium for providing resources and support. This work was supported in part by the Offices of NP and HEP within the U.S. DOE Office of Science, the U.S. NSF, the Sloan Foundation, the DFG cluster of excellence ‘Origin and Structure of the Universe’ of Germany, CNRS/IN2P3, FAPESP CNPq of Brazil, Ministry of Ed. and Sci. of the Russian Federation, NNSFC, CAS, MoST, and MoE of China, GA and MSMT of the Czech Republic, FOM and NWO of the Netherlands,

DAE, DST, and CSIR of India, Polish Ministry of Sci. and Higher Ed., Korea National Research Foundation, Ministry of Sci., Ed. and Sports of the Rep. of Croatia, and RosAtom of Russia.

-
- [1] T. Matsui and H. Satz, Phys. Lett. **B178**, 416 (1986).
 - [2] S. Digal, P. Petreczky, and H. Satz, Phys. Rev. **D64**, 094015 (2001).
 - [3] F. Karsch, D. Kharzeev, and H. Satz, Phys. Lett. **B637**, 75 (2006).
 - [4] A. Mocsy and P. Petreczky, Phys. Rev. Lett. **99**, 211602 (2007).
 - [5] A. Mocsy and P. Petreczky, Phys. Rev. **D77**, 014501 (2008).
 - [6] N. Brambilla et al., Eur. Phys. J. **C71**, 1534 (2011).
 - [7] M. C. Abreu et al., Phys. Lett. **B499**, 85 (2001).
 - [8] A. Adare et al., Phys. Rev. Lett. **98**, 232301 (2007).
 - [9] G. Aad et al., Phys. Lett. **B697**, 294 (2011).
 - [10] S. Chatrchyan et al., JHEP **1205**, 063 (2012).
 - [11] B. Abelev et al. (2012), arXiv:1202.1383.
 - [12] F. Karsch and R. Petronzio, Phys. Lett. **B193**, 105 (1987).
 - [13] Y.-p. Liu, Z. Qu, N. Xu, and P.-f. Zhuang, Phys. Lett. **B678**, 72 (2009).
 - [14] X. Zhao and R. Rapp, Phys. Rev. **C82**, 064905 (2010).
 - [15] H. Liu, K. Rajagopal, and U.A.Wiedemann, Phys. Rev. Lett. **98**, 182301 (2007).
 - [16] R. Sharma and I. Vitev (2012), arXiv:1203.0329.
 - [17] B. I. Abelev et al., Phys. Rev. **C80**, 041902 (2009).
 - [18] W. Llope et al., Nucl. Instrum. Meth. **A522**, 252 (2004).
 - [19] M. Beddo et al., Nucl. Instrum. Meth. **A499**, 725 (2003).
 - [20] B. Abelev et al., Phys. Rev. **C79**, 034909 (2009).
 - [21] A. Adare et al., Phys. Rev. **D82**, 012001 (2010).
 - [22] M. Anderson et al., Nucl. Instrum. Meth. **A499**, 659 (2003).
 - [23] Z. Tang, Ph.D. thesis, University of Science and Technology of China (2009), URL http://drupal.star.bnl.gov/STAR/files/Tang_Zebo.pdf.
 - [24] B. Bonner et al., Nucl. Instrum. Meth. **A508**, 181 (2003).
 - [25] J. Adams et al., Phys. Rev. Lett. **94**, 062301 (2005).
 - [26] J. Adams et al., Phys. Lett. **B616**, 8 (2005).
 - [27] J. Adams et al., Phys. Rev. **C71**, 064902 (2005).
 - [28] Z. Tang, Nucl. Phys. **A855**, 396 (2011).
 - [29] J. Adams et al., Phys. Rev. Lett. **91**, 172302 (2003).
 - [30] K. Nakamura et al. (Particle Data Group), J. Phys. G **G37**, 075021 (2010), Branching ratio for $J/\psi \rightarrow e^+e^-$ is $(5.94 \pm 0.06)\%$, including $(0.88 \pm 0.14)\%$ for $J/\psi \rightarrow \gamma e^+e^-$.
 - [31] Y.-Q. Ma, K. Wang, and K.-T. Chao, Phys. Rev. **D84**, 114001 (2011), and private communication (2012). The color-octet model describes the J/ψ production process as having the quantum number of the color configuration at the intermediate state different from that of the J/ψ .
 - [32] A. D. Frawley, T. Ullrich, and R. Vogt, Phys. Rept. **462**, 125 (2008), and R. Vogt private communication (2009). The color evaporation model is motivated by the principle of quark-hadron duality. It assumes that every produced $c\bar{c}$ evolves into charmonium if it has an invariant mass less than the threshold for producing a pair of open charm mesons. The nonperturbative probability for the $c\bar{c}$

- to evolve into a charmonium state is given by an energy-momentum and process independent constant.
- [33] P. Artoisenet et al., Phys. Rev. Lett. **101**, 152001 (2008), and J.P. Lansberg private communication (2009). The color-singlet model describes the J/ψ production process as having the quantum number of the color configuration at the intermediate state the same as that of J/ψ .
 - [34] T. Sjostrand, S. Mrenna, and P. Skands, JHEP **05**, 026 (2006).
 - [35] T. Sjostrand, S. Mrenna, and P. Z. Skands, Comput. Phys. Commun. **178**, 852 (2008).
 - [36] M. Bedjidian et al., hep-ph/0311048 and R. Vogt private communication (2004).
 - [37] M. Cacciari, P. Nason, and R. Vogt, Phys. Rev. Lett. **95**, 122001 (2005).
 - [38] Z. Xu, Y. Chen, S. Kleinfelder, A. Koohi, S. Li, et al. (2006), LBNL-PUB-5509.
 - [39] S. Margetis, Nucl. Phys. B (Proc. Suppl.) **210-211**, 227 (2011).
 - [40] D. E. Acosta et al., Phys. Rev. **D71**, 032001 (2005).
 - [41] G. Aad et al., Nucl. Phys. **B850**, 387 (2011).
 - [42] V. Khachatryan et al., Eur. Phys. J. **C71**, 1575 (2011).
 - [43] Z. Tang et al., Phys. Rev. **C79**, 051901 (2009).
 - [44] Z. Tang et al. (2011), arXiv:1101.1912.
 - [45] G. Agakishiev et al., Phys. Rev. Lett. **108**, 072302 (2012).
 - [46] B. Abelev et al., Phys. Rev. Lett. **97**, 152301 (2006).
 - [47] A. G. Clark et al., Phys. Lett. **B74**, 267 (1978).
 - [48] A. L. S. Angelis et al., Phys. Lett. **B79**, 505 (1978).
 - [49] Y. Liu, N. Xu, and P. Zhuang, Nucl. Phys. **A834**, 317c (2010).